Experiments on *Pause and Go* State Estimation and Control with Uncertain Sensors Feedback

Violet Mwaffo[1(✉)], Jackson S. Curry[2], Francesco Lo Iudice[3], and Pietro DeLellis[3]

[1] United States Naval Academy, Annapolis, MD, USA
mwaffo@usna.edu
[2] University of Colorado Boulder, Boulder, CO, USA
jackson.curry@colorado.edu
[3] University of Naples Federico II, Naples, Italy
{francesco.loiudice,pietro.delellis}@unina.it

Abstract. A bio-inspired state estimation and control algorithm is experimentally tested to autonomously balance a team of robots on a circle. In this control scheme inspired from the social behavior of some insects species, a leader is elected randomly and periodically moves at a constant angular speed. The followers triggered by the leader motion, implement a decentralized and non-cooperative state estimation and control algorithm using uncertain and noisy proximity sensor measurements. Individuals in the team are immobile during the *pause* sequence to gather and process proximity distances, identify closer neighbors, and estimate their relative phase distances. During the *go* sequence, they either accelerate to achieve the desired spacing from closer neighbors, or move at a constant angular speed in phase with the leader. The scheme is tested on caster wheeled robots equipped with a rotating sonar platform to get forward and backward distances and is shown capable to balance the team of robots even in the presence of false readings or intermittent measurements. Further, at steady-state, the team of robots is capable to self balance in the absence of sensor feedback.

Keywords: Bio-inspired · State estimation and control · Autonomous systems

1 Introduction

Coordinating multiple vehicles is becoming pervasive for potential applications in collective search and rescue missions [3], disaster relief and management

Supported by the United States Naval Academy and by the program "STAR 2018" of the University of Naples Federico II and Compagnia di San Paolo, Istituto Banco di Napoli - Fondazione, project ACROSS.

T. Nakano (Ed.): BICT 2021, LNICST 403, pp. 87–101, 2021.
https://doi.org/10.1007/978-3-030-92163-7_8

systems [18], and surveillance and reconnaissance missions [1]. To achieve the autonomous coordination of multiple vehicles, formation control algorithms have explored path or way points tracking [28], patterns configuration [25], or moving through constrained environment [8]. Among the existing algorithms, leader-follower formation control schemes [7] are popular and cost-efficient. Leader-follower relationships are commonly hypothesized to be fundamental in explaining the emergence of collective behaviour in several natural organisms. Indeed, leaders are often considered as informed individuals guiding other group members toward set locations. In insect groups for example, leadership might benefit the group during foraging or migration [10]. As such, leaders-followers relationships are central to the understanding of the interaction between group members. For robotic applications, only a handful of agents, denoted leaders, need to utilize navigation tools such as Simultaneous Localization and Mapping (SLAM) [23] or Differential Global Positioning System (DGPS) [11] to drive the followers towards the desired path, whereas the followers only rely on cheap proximity sensors such as sonar, infrared, or camera to stay aligned with the rest of the team. These sensors have very short range and their performance might significantly deteriorate in changing or cluttered environments [26].

For real world applications, decentralized and local communication protocols are often preferred to centralized approaches as they typically require less computation resources and sensing capabilities [16]. In case of limited communication due to cluttered environments or the medium restraining wireless communications, each robot has to rely on its own sensing capabilities [21]. To improve the accuracy of both relative and absolute localization methods, research efforts have proposed robust estimation methods [5], non-linear Kalman filter [19], or the use of diversified pool of sensors [22]. In localization problems [20], individual robots have to independently regulate their dynamics using either relative positions with respect to internal kinematics [9], or absolute position with respect to a reference frame [19]. In these problems, few works have addressed the case of the absent or intermittent feedback data that might arise when proximity sensors are employed, in the presence of a cluttered environment, in underwater applications, or in case of varying light or air conditions [4].

Here, we depart from a bio-inspired estimation and control scheme [24] and illustrate how a recent state estimation and control algorithm [12,13] can be implemented on ground robots. Specifically, here we focus on the cheapest implementation in which the robots are equipped with ultrasonic sensors, whose limited accuracy need to be compensated by a synergistic design of the estimator and controller. The team of robots includes a single leader and several followers implementing the state estimation and control algorithm based on noisy and intermittent proximity distances to predict their relative position with their closest pursuant on the circle. This decentralized non-cooperative approach is implemented in a *pause-and-go* scheme, where, during the *pause*, followers recursively estimate their relative angular position to the robot ahead or behind on the circle and during the *go*, followers either accelerate or move at a constant speed to appropriately space from nearby robots. The *pause-and-go* behavior has been

observed in some insect species [2] that adopt this strategy during foraging or social interaction, or to better appreciate the closeness or the alignment to a distant target or to a conspecific [27].

Outline of the Paper: Section 2 describes the formation control problem and the state estimation and control algorithm. Section 3 depicts the experimental setup and the trials. Section 4 present the results and Sect. 5 concludes the work.

2 State Estimation and Control Algorithm

2.1 Problem Statement

We consider a group of $i = 1, ..., N$ mobile robots moving on a circle of radius $R > 0$ and updating their angular position $\theta_i(k)$ at each discrete time instant k as:

$$\theta_i(k+1) = \begin{cases} \theta_i(k) + u_i(k), & \text{if } (k/p) \in \mathbb{N}, \\ \theta_i(k), & \text{otherwise,} \end{cases} \tag{1}$$

where $u_i(k)$ is the control input implemented in a *pause-and-go* fashion and $p \in \mathbb{N}$ is an integer corresponding to the number of time steps needed to perform the measurements and estimations.

The control goal is to find $u_i(k)$ in order to set the pace of the group to the a desired angular speed ω_{ref} every p time steps, and coordinate the team of robots in a balanced formation on the circle. Formally, this translates into achieving an ε bounded formation [21], that is,

$$\limsup_{k \to +\infty} |\xi_{ij}(k) - 2\pi/N| \leq \varepsilon, \tag{2}$$

for given any pair of consecutive agents (i, j), where $\xi_{ij}(k) := \text{rem}(\theta_i(k) - \theta_j(k))$ is the relative phase between robots i and j[1]; the quantity $2\pi/N$ is the desired angular spacing between consecutive agents, and ε is the formation error.

For the team of robots defined above, we consider the challenging scenario where (i) each robot is equipped with a proximity sensor with a limited range r_v that corresponds to a *visibility cone* $\varphi_v = 2\arcsin(\rho_v/2R)$ along the circle; (ii) the on-board computer power can only allow to collect intermittent measurements every p steps, where p is the time required to acquire and to process the information; (iii) each robot, say i, obtains a noisy measurement $\tilde{d}_{ij}$ (affected by a bounded noise δ_{ij}) of the distance d_{ij} from a robot $j \neq i$ only if $d_{ij} \leq r_v$; (iv) the robots have no mean to uncover the identity and relative order (ahead or behind)[2] with respect to closer neighbors.

The above constraints imply that pairwise proximity distance satisfies:

$$\tilde{d}_{ij}(k) = \begin{cases} d_{ij}(k) + \delta_{ij}(k), & \text{if } d_{ij}(k) \leq r_v \wedge (k/p) \in \mathbb{N}, \\ \text{n.a.}, & \text{otherwise,} \end{cases} \tag{3}$$

[1] $\text{rem}(z)$ denotes the unique solution for r to the equation $z = 2\pi w + r$, where $-\pi \leq r < \pi$, $w \in \mathbb{Z}$.

[2] We say that robot i is ahead of j at time k if $\xi_{ij}(k) > 0$, otherwise i is behind j.

where the measurement error verifies $|\delta_{ij}| \leq \delta_{\max}$ for a given positive scalar $\delta_{\max}$, and n.a. stands for no measurement available. We comment that the control objective in (2) cannot be fulfilled by traditional control schemes considering the limitations on the available measurements summarized by Eq. 3.

Introducing the relative phase distance $\varphi_{ij}(k) := |\xi_{ij}(k)|$ between robots i and j, from Eq. (3), we know that[3]

$$\varphi_{ij}(kp) \in \begin{cases} \Upsilon_{ij}(kp), & \text{if } \varphi_{ij}(kp) \leq \varphi_v, \\ \overline{\Upsilon}, & \text{otherwise,} \end{cases} \tag{4}$$

where $\overline{\Upsilon} := (\varphi_v, \pi]$, and

$$\Upsilon_{ij}(kp) := [\max\{\tilde{\varphi}_{ij}(kp) - \varphi_{\max}, 0\}, \min\{\tilde{\varphi}_{ij}(kp) + \varphi_{\max}, \varphi_v\}], \tag{5}$$

with $\tilde{\varphi}_{ij}(kp) = 2\arcsin(\tilde{d}_{ij}(kp)/2R)$ defining the phase distance corresponding to the measured Euclidean distance $\tilde{d}_{ij}(kp)$; $\varphi_{\max} := 2\arcsin((r_v + \delta_{\max})/2R) - 2\arcsin(r_v/2R)$ is the maximum uncertainty associated to $\tilde{\psi}_{ij}(kp)$. Note that from (4), albeit the relative position of the closer robot is unknown, we are aware that ξ_{ij} belongs to two uncertainty intervals (one in $[0, \pi)$ and the other in $[-\pi, 0)$) with width $\Gamma_1^{ij}(kp)$ and $\Gamma_2^{ij}(kp)$. Using the information coming from (4) and the knowledge of individual dynamics in (1), it is possible to shrunk the width of these uncertainty intervals. Note that the hull $H_{ij}(kp)$ of the multi-interval $\Gamma_{ij}(kp) = \Gamma_1^{ij}(kp) \cup \Gamma_2^{ij}(kp)$ is an overestimate of the uncertainty on $\xi_{ij}(kp)$. The reader can refer to [21] for basic properties and operations on intervals, which will be used when designing the control and estimation strategy presented below.

2.2 Control Strategy

Here, we leverage the synergistic control and estimation strategy first proposed in [21], which prescribes the random election of a leader, w.l.o.g. a robot, whose control law $u_1(k) = \omega_{\text{ref}}$, and thus sets the pace for the multi-agent system, while the followers $i = 2, ..., N$ implement a three-level bang-bang control law with initial value $u_i(0) = 0$. Initially, none of the robots is in the visibility range of another robot, the relative motion of the leader will determine a time-instant in which it will enter the *visibility cone* of robot $i = 2$. In that case, robot $i = 2$ starts implementing a prediction-correction algorithm to obtain an estimate $\hat{\Theta}_{21}$ of the relative phase ξ_{12}. Using this estimate, the control strategy can be activated resulting is either one of these two actions:

1. if node 1 is closer than the desired spacing $2\pi/N$, the control law u_2 is set to $\omega_{\text{ref}} + c$, with $c > 0$ introduced to move robot 2 faster than the leader, thereby incrementing the spacing distance between nodes 1 and 2;

[3] For simplicity, given the *pause-and-go* implementation, the measured distance and related quantities will be only defined at time instants kp, with k being an integer.

2. if the desired distance is achieved, the control input u_2 is switched to the desired speed ω_{ref}.

In turn, robot $i = 2$ while moving will eventually enters the *visibility cone* of robot 3 resulting into a sequential repetition of the above steps for all pairs of consecutive robots until the ε-balanced formation is achieved.

Note that at time kp, robot i possesses an interval estimate $H_{ij}(kp|kp)$[4] of the relative phase angle $\Theta_{ij}(kp)$ with respect to neighbors robot j. Introducing $\underline{H}$ and $\bar{H}$ as the infimum and supremum of an interval H respectively, at time kp, when the conditions

$$\begin{aligned} &\underline{H}_{i,i-1}(kp|kp) > 0, \\ &\bar{H}_{i,i-1}(kp|kp) < \underline{\Gamma}_1^{ij}(kp|kp), \text{for all } j \neq i-1 \end{aligned} \tag{6}$$

are both satisfied, robot i can unambiguously concludes that $j = i - 1$ is its closest pursuant.

The multi-level control strategy implemented by the team of robots can be summarized at any time instant k as:

$$u_1(k) = \omega_{\text{ref}}, \qquad \text{for leader } i = 1 \tag{7a}$$

$$u_i(k) = \begin{cases} \omega_{\text{ref}} + c\,, & \text{if } \hat{\Theta}_{i,i-1}(k) < 2\pi/N \text{and } k \geq k_i, \\ \omega_{\text{ref}}\,, & \text{if } \hat{\Theta}_{i,i-1}(k) \geq 2\pi/N \text{and } k \geq k_i, \\ 0, & \text{otherwise,} \end{cases} \quad \text{for followers } i \geq 2 \tag{7b}$$

where k_i is the first time-instant that robot i is capable to identify its closest pursuant, that is, the first time instant such that (6) holds, and for any $i = 2, \ldots, N$, $\hat{\Theta}_{i,i-1}(k)$ is selected as $\bar{H}_{i,i-1}(\lfloor k/p \rfloor | \lfloor k/p \rfloor)$. In what follows, we introduce the estimation strategy to update the multi-interval $\Gamma_{ij}(kp|kp)$ upon which H_{ij} is computed.

2.3 Estimation Algorithm

The estimation strategy leverages the three-level bang-bang structure of the control law to perform an interval estimate $\hat{u}_j^i(k)$ of the input acting on node $i \geq 2$ at time k as:

$$\hat{u}_j^i(k) = \begin{cases} \omega_{\text{ref}}, & \text{if } k \geq k_i, d_{ij} > r_v, j = i-1, \\ [\omega_{\text{ref}}, \omega_{\text{ref}} + c], & \text{if } k \geq k_i, d_{ij} \leq r_v, j = i-1, \\ [0, \omega_{\text{ref}} + c], & \text{otherwise.} \end{cases} \tag{8}$$

Each robot requires p time instants to process the measurements and compute the next control input, thereby the uncertainty on the interval estimation of ξ_{ij}, denoted Γ_{ij}, is updated every p steps using (4) for all $i = 2, \ldots, N, j \neq i$ starting from the initialization $\Gamma_{ij}(0|-p) = [-\pi, \pi)$ as:

[4] The notation $|kp$ indicates that agent i has used all information collected until kp.

$$\Gamma_{ij}(kp|kp) = \begin{cases} \emptyset, & \text{if } kp \geq k_i, j \neq i-1, \\ \Gamma_{ij}(kp|(k-1)p) \cap \left(\overline{\Upsilon} \cup -\overline{\Upsilon}\right), & \text{if } kp \geq k_i, d_{ij}(kp) > \rho_v, j = i-1, \\ \overline{\Upsilon} \cup -\overline{\Upsilon}, & \text{if } kp < k_i, d_{ij}(kp) > \rho_v, \\ \Gamma_{ij}(kp|(k-1)p) \cap (\Upsilon_{ij}(kp) \cup -\Upsilon_{ij}(kp)), & \text{otherwise}, \end{cases} \tag{9}$$

for all $k > 0$. Equation (9) prescribes that, prior to time instant k_i, when no measurement is available, robot i does not evaluate the intersection $\Gamma_{ij}(kp|(k-1)p) \cap (\Upsilon_{ij}(kp) \cup -\Upsilon_{ij}(kp))$. Thus, when $d_{ij}(kp) > r_v$, robot i just sets $\Gamma_{ij}(kp|kp) = (\Upsilon_{ij}(kp) \cup -\Upsilon_{ij}(kp))$. After time k_i, robot i stops estimating the position of all other agents except its closest pursuant $i-1$.

Algorithms 1 and 2 report a schematic implementation of the estimator (9). The uncertainty interval $\Gamma_{ij}(kp|kp)$ is recursively estimated p steps ahead as:

$$\Gamma_{ij}((k+1)p|kp) = \Gamma_{ij}(kp|kp) + \hat{u}_{ij}(kp), \text{ for all } j \neq i, \tag{10}$$

where robot i's estimate of the relative input with respect to j is $\hat{u}_{ij}(kp) := u_i(kp) - \hat{u}_j^i(kp)$ where $\hat{u}_j^i(kp)$ is given in (8).

The convergence of the *pause-and-go* estimation and control strategy is a particular case of the algorithm proposed in [21] and the convergence of the proposed scheme can be established using a similar procedure as in [21] while taking into account the periodical activation of the control scheme defined in (7a)–(10). In particular, an upper bound $\tilde{k}_i$ of the convergence time k_i can be determined.

Proposition 1 [24]**.** *For the multi-robot system in* (1)*, If*

1. $|\Theta_{ij}(0)| \in [\min\{4\varphi_{\max} + 2\omega_{\text{ref}} + 2c, \varphi_v\}, \pi]$, *for all* $i = 1, \ldots, N$, $i \neq j$;
2. $2(\omega_{\text{ref}} + c) < \varphi_v$;
3. $\omega_{\text{ref}} > 0$ *and* $0 < c < \epsilon/(N-1)$,

then there exist $k_2, \ldots, k_N < +\infty$. *In addition,* $k_i \leq \tilde{k}_i$, *where*

$$\tilde{k}_i = \begin{cases} p\left\lceil (\theta_2(0) - \theta_1(0) - 2(\omega_{\text{ref}} + c))/\omega_{\text{ref}} \right\rceil, & \text{if } i = 2, \\ k_{i-1} + p\left\lceil (\Theta_{i,i-1}(0) - \varphi_v)/\omega_{\text{ref}} \right\rceil, & \text{if } i \neq 2 \wedge \Theta_{i,i-1}(0) > \varphi_v, \\ k_{i-1} + p\left\lceil (\theta_i(0) - \theta_{i-1}(0) - \varphi_v)/\omega_{\text{ref}} \right\rceil, & \text{if } i \neq 2 \wedge \Theta_{i,i-1}(0) < 0, \\ k_{i-1} + p\left\lceil (\Theta_{i,i-1}(k_{i-1}) - 4\varphi_{\max})/\omega_{\text{ref}} \right\rceil, & \text{otherwise.} \end{cases} \tag{11}$$

The results in [21] has also been adapted to provide sufficient conditions to achieve a ε-balanced formation in the *pause-and-go* estimation and control strategy can be obtained as

Proposition 2 [24]. *For the multi-robot system* (1)*, If there exist* $\varepsilon > 0$ *such that:*

1. $|\Theta_{ij}(0)| \in [\min\{4\varphi_{\max} + 2\omega_{\text{ref}} + 2c, \varphi_v\}, \pi]$, *for all* $i = 1, \ldots, N$, $i \neq j$;
2. $2(\omega_{\text{ref}} + c) < \varphi_v$;
3. $\omega_{\text{ref}} > 0$ *and* $0 < c < \varepsilon/(N-1)$;

then (i) the estimation and control strategy in (7a)–(10) *achieve a* ε*-balanced formation, that is* $\lim_{k \to +\infty} |\Theta_{i,i+1}(k) - 2\pi/N| \leq c$, *and in addition, (ii) the relative phase* $\Theta_{i,i+1}(k)$ *converges in finite time* $k_i^c \leq \bar{k}_i^c$ *for a given* $k_i^c \in \mathbb{N}$, *for all pair of robots* $(i, i+1)$ *with* $i = 1, ..., N-1$.

Remark 1. From the above propositions, the control parameter c can be carefully selected to regulate the trade-off between accuracy and convergence speed. In particular, smaller values of c might improve the accuracy of the control scheme while increasing the convergence time. This is in particular true for larger group sizes where individuals might be required to move at a slow pace to avoid collision or motion jamming. However, for larger team sizes, it is more likely that individual robots can perceive each other, hindering a key feature of our control scheme which assumes that, at steady state, the range of visibility is lower than the desired spacing distance. Note that, in that case, alternative approaches such as the control scheme proposed in [13] could be utilized.

Remark 2. In case a single or more agents N_r are forced to leave the formation, the algorithm can still converges if the rest of robots are informed of the new desired spacing $2\pi/(N - N_r)$. As the leader is randomly elected, a fault affecting the leader is not critical to the proposed startegy.

3 Experiments

3.1 Hardware

A custom made castor wheeled robotic platform equipped with an ultrasonic sensor is utilized in the experiments. The ultrasonic sensor is mounted on a *servo motor* allowing to rotate the device and to measure frontward or backward proximity distance. The analog signal of the ultrasonic sensor is processed by an *Arduino Uno* micro-controller. The state estimation and control algorithm was written with custom python code and run by a Raspberry Pi computer board interfaced through serial communication with the micro-controller to receive sensor data.

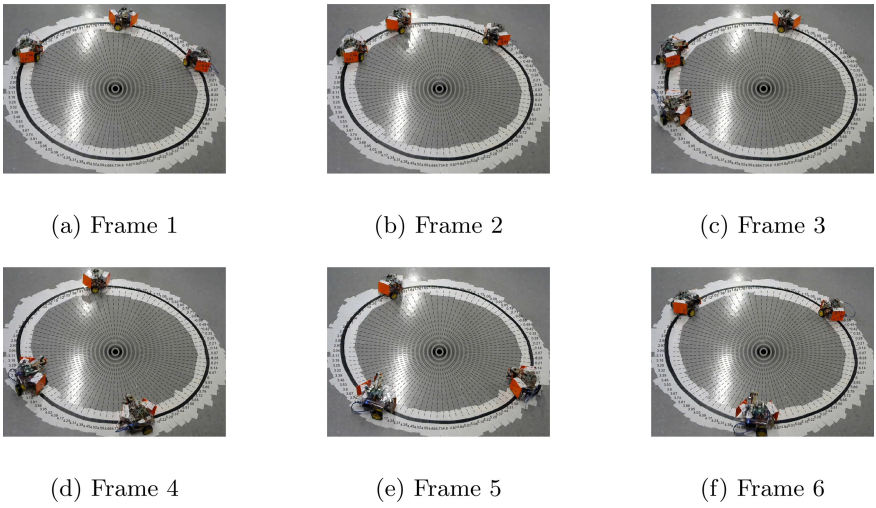

(a) Frame 1 (b) Frame 2 (c) Frame 3

(d) Frame 4 (e) Frame 5 (f) Frame 6

Fig. 1. A sequence of snapshots, sampled at intervals of 200 s, of a sample trial with a team of three robots achieving a circular self-balancing formation.

The *servo-motor* was also set to position the sensor either frontward and backward at three different angular position values spaced by an angle of $7\pi/36$ rad. At each of these positions, eight different measurements were taken and only values between 0.05 m and the circle's diameter were considered and their median computed as the proximity distance to inform the algorithm. Note that, these multiple measurements allowed to compensate for the reduced accuracy of the ultrasonic sensor when the object detected is not directly aligned with the sensor. To fulfill with the constrained imposed to the state estimation and control algorithm, we set the code to discard measurement values greater than a meter yielding to a maximum proximity radius in the output Eq. (3) of $r_v = 1$ m and corresponding to a visibility angle of $\varphi_v = 1.59$ rad.

The robots were programmed to move on a circle identified by a narrow black adhesive tape on top of a wider white adhesive tape. Custom python scripts implementing an independent PID control algorithm with feedback from encoders mounted on the wheels and from the light sensors was utilized to maintain the robot along the black stripe. The radius of the circle was set to $R = 0.7$ m in order to maintain a blind sensing spot of about $\pi/6$ rad prior to reaching the balanced circular formation. The line following algorithm was observed to result in a zig-zag motion generating additional disturbances to the formation control algorithm.

3.2 Procedure

The experiments were performed with group of three robots. A single robot was set as the leader to move at a constant reference angular speed ω_{ref}. All robots,

including the leader, were equipped with the ultrasonic sensor not to detect and estimate proximity distance, but also to avoid possible collision with neighbors. This procedure was necessary in case a robot ahead of the team become faulty or unresponsive. We comment that, when the algorithm is successfully implemented by all robots, collision avoidance is useless as the closest robot will detect the motion of the pursuant and initiate its own motion. Further, as the followers rely solely on proximity distances and do not communicate with closer neighbors, a key feature of the state estimation and control algorithm in (6)–(10) is to be fully decentralized and non-cooperative.

The initial position of the robot was set to ensure that two consecutive robots could not detect each other at the beginning of the experiments. Prior to the experiments, pilot trials were conducted allowing to set the pause time interval duration to 55 s. Given that the duration of each time step in Eq. (1) is 1 s, the number of time steps required to *pause* is $p = 55$. Five experimental trials were performed for a total duration of 25 min each. The trials were video recorded using an overhead camera to obtain a wide complete view of the arena. The motion of each robot was then manually extracted from the video frames using a protractor superimposed on top of each picture frames (see Fig. 1).

3.3 Control Parameters

We set the reference angular speed to $\omega_{\text{ref}} = 0.1$ rad/s and we select the control parameter c such that the ε-balanced formation is achieved by the team of robots with a maximum formation error $\varepsilon = 0.4$ rad. Given the trade-off between convergence speed and accuracy (see Remark 1), we select $c = 0.2$ rad/s which is compatible with the maximum formation error above while allowing to fulfill the hypothesis of Propositions 1 and 2. This can be verified for each pair of consecutive agents i and j by evaluating $\varphi_{ij}(0) \in [0.84, 2.02[\subset [\min\{4\varphi_{\max} + 2\omega_{\text{ref}} + 2c, \varphi_v\}, \pi] = [0.68, \pi]$[5], and $\omega_{\text{ref}} + c = 0.3$ rad $< \varphi_v = 1.59$ rad.

4 Results

4.1 Proximity Distances

Table 2 in Appendix presents the raw data estimates of the phase angles measure with the ultrasonic sensors in consecutive iterations after p time steps each. The presence of missing values denoted "n.a." in the Table indicates that the ultrasound sensor often does not return meaningful measurements. In particular, at steady state, measurements might not be available as the desired spacing distance is set at $2\pi/N = 2\pi/3 \simeq 2.09$ rad, much larger than the *visibility cone* that corresponds to a threshold value of $\varphi_v = 1.59$ rad. In the Table, the existence of a measurement value for the backward sensor reading value of robot 1 also indicates that the sensor might also return false readings due to occasional

[5] Note that $\varphi_{\max} = 4.2 \times 10^{-2}$ rad since $\delta_{\max} = 0.02$ m. The relationship between $\varphi_{\max}$ and $\delta_{\max}$ is given below Eq. (5).

obstructions of the signal by the operator conducting the experiments. Further, the multiplicity of sound wave emitted by several robots might overlap as the micro-controller cannot differentiate them. As such the control scheme has to deal with additional sources of uncertainties.

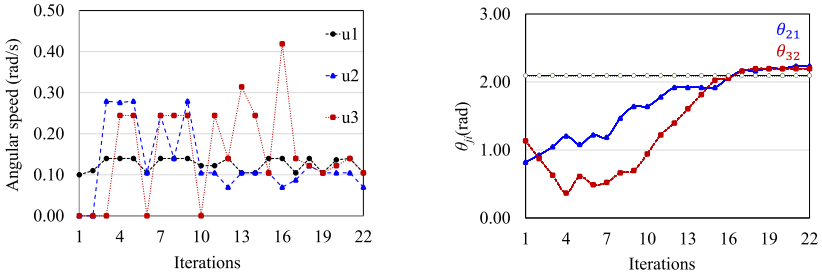

Fig. 2. Evolution of the control law u_i in (7a)–(7b) (left panel) and relative phase angle difference between robots 2 and 1 and between robots 3 and 2 (red panel) in consecutive iterations (every p time steps) for an exemplary trial. The dash-dotted horizontal line in the right panel corresponds to the desired spacing phase angle $2\pi/3$ (Color figure online)

4.2 Control Actuation

The left panel of Fig. 2 depicts the time trace of the control output u_1, u_2, and u_3 observed for each robot. Robots 2 and 3 are able in a few iterations to identify the presence of their closest pursuant by setting their values to 0.3 rad/s in order to space accordingly. We note that the values observed are often different from the control input which should be either 0 initially, then 0.3 rad/s when the motion is initiated, and 0.1 rad/s when the desired spacing is achieved. Note that the large fluctuations of the observed angular speed are explained by several factors including the zig-zagging line following motion, slip, friction, or inaccurate encoder feedback.

Table 1. Convergence rate measured by the number of iterations for robot between robots i to achieve the desired spacing (k_i^c/p), steady-state relative phase angle ($\bar{\Theta}_{ij}$) and maximum formation error ($|\bar{\Theta}_{ij} - \frac{2\pi}{3}|$) between robots i and j. "se" is the standard error.

Measure	k_i^c/p			$\Theta_{i,i-1}$ (rad)		$\lvert\bar{\Theta}_{i,i-1} - \frac{2\pi}{3}\rvert$
Statistics	min	mode	max	mean (rad)	se (rad)	max (rad)
Robot 2	6	7	7	2.02	0.15	0.23
Robot 3	11	11	14	2.20	0.24	0.29

4.3 Convergence

Table 1 presents relevant data of the self-balancing convergence including the number of iterations implemented by a follower robot to reach the desired spacing distance, the averaged relative phase distance between robots, and the maximum formation error observed. The Table shows that the first follower achieves the desired spacing in about 7 iterations while the second robot needs about 11 iterations to converge. The estimated balancing error is always less than 0.30 rad corresponding to the maximum angle value $\omega_{\text{ref}} + c$ spanned by the robot in a single step. This value is also less than the predicted maximum error value 0.40 rad from Proposition 2. In addition, each follower is observed to identify their closest pursuant in a single iteration. Note that the upper bound predicted by (11) is $k_2/p = 3$ and $k_3/p = 10$ for robot 2 and robot 3 respectively.

The right panel of Fig. 2 depicts the time trace of the relative phase angle difference between robot 2 and robot 1 and between robots 3 and robot 2. In the figure, as time evolves, both values tend to converges toward the desired spacing value $2\pi/N = 2\pi/3 = 2.09$ rad in about 14 iterations. Note that, as discussed in Remark 1, by further reducing the value of the control parameter c, one might further increase the accuracy of the state estimation and control scheme.

5 Conclusion

A non-cooperative and fully decentralized state estimation and control scheme has been experimentally tested. Inspired by the behavior of insects, which stop to enhance the effectiveness of their next move, the scheme is implemented in an *pause-and-go* fashion on a low cost robotic platform consisting of three castor wheeled robots. It relies on uncertain and intermittent proximity distances measured by an ultrasonic sensor. The estimation and control strategy is capable to autonomously space the robots' along the circle even in case the sensor range is shorter than the desired spacing. By means of a suitable selection of the main control parameters, it is possible to drive the formation error below a desired threshold value and to regulate the trade-off between accuracy and convergence speed. Further, we illustrated that a low-cost implementation of this strategy is robust enough to handle occasional false readings and inaccuracies of the ultrasound sensor. These promising results showing robustness to noise and uncertainties make the proposed approach particularly suitable for applications such as distributed sensor placements or coverage control problems [15]. The proposed state pause-and-go implementation well fits low costs micro-robotic applications that are not time-critical but require limited payload and accuracy. Within formation control problems, the proposed formulation on the circle is relevant to problems such as perimeter surveillance [17] and source seeking [6], and can be possibly extended to more complex shapes assuming they can be approximated with Jordan curves [14]. Depending on the application and on the available budget, different kind of sensors can be employed, see e.g. the discussion in [24] for alternative sensor selections.

Acknowledgments. The authors are grateful to Samuel Coyle and Kevin Lee for contributing during the Summer Program for Undergraduate Research (CU SPUR 2018) in preliminary works to design and fabricate the robotic platform.

Author contributions. V.M., P.D., and F.L.I. designed the study, J.S.C. conducted the experiments on ground robots, V.M., P.D., F.L.I., and J.S.C. performed the analysis, V.M., and P.D. wrote the manuscript, with contributions from all authors.

6 Appendix

Table 2. Proximity distances in radiant (rad) measured frontward and backward by the ultrasonic sensor in an exemplary trial. Note that in case of no measurement or no object detected within the sensing range, the estimated proximity distance is set to "n.a." as in (3). False readings are inside a box.

Iteration	Back 1	Front 1	Back 2	Front 2	Back 3	Front 3
1	n.a.	1.13	n.a.	n.a.	n.a.	n.a.
2	n.a.	n.a.	0.87	2.42	2.12	n.a.
3	n.a.	n.a.	1.61	n.a.	1.34	n.a.
4	n.a.	1.43	n.a.	1.74	0.79	n.a.
5	n.a.	n.a.	n.a.	1.03	1.30	n.a.
6	1.30	n.a.	n.a.	1.06	0.93	n.a.
7	n.a.	n.a.	n.a.	1.11	0.76	n.a.
8	0.85	n.a.	1.29	n.a.	0.84	2.09
9	n.a.	n.a.	n.a.	1.03	1.16	2.38
10	n.a.	n.a.	n.a.	n.a.	1.42	n.a.

Algorithm 1. Implementation of the state estimation in (9). $\lambda(k)$ refers to the number of intervals in $J(k) = -\Upsilon_{ij}(kp) \cup \Upsilon_{ij}(kp)$ and the subroutine Evaluate is defined in Algorithm 2.

procedure INITIALIZATION ($k = 0$, $k_i < 0$) ▷ Initially set time $k = 0$ and $k_i < 0$
  $J_l(k) = \Upsilon_{ij}(k) \cup -\Upsilon_{ij}(k)$ ▷ Evaluate $J_l(0)$
  if $\Theta_{ij}(0) \leq \varphi_v$ **then** ▷ i can detect j
    $k_i = 0$ ▷ set $k_i = 0$
  end if
  while width$(H(kp)) \geq \delta$ **do** ▷ δ is to be defined
    $[\lambda(k), J_l(k)] \leftarrow$ Evaluate$\{J_l(k-1) \cap \Gamma_{ij}(kp|(k-1)p)\}$
    if $\tilde{d}_{ij}(kp) \neq$ n.a. **then** ▷ A value is returned
      if $k_i < 0$ **then**
        $k_i = kp$
      end if
    else ▷ No value is returned
      if $\varphi_v \leq \frac{\pi}{3}$ **then**
        $\lambda(k) = 2$ ▷ $\Gamma_{ij}(kp|kp)$ has two intervals
      else
        $\lambda(k) \leq 1$ ▷ $\Gamma_{ij}(kp|kp)$ is either the empty set or a single interval
      end if
    end if
    $k = k + 1$
    $J_l(k) = -\Upsilon_{ij}(kp) \cup \Upsilon_{ij}(kp)$
    width $(H(kp)) = \max_l J_l(k) - \min_l J_l(k)$
  end while
  return $J_l(k|k)$
end procedure

Algorithm 2. Subroutine of Algorithm 1.

procedure
  Evaluate$\{J_l(k|k-1) \cap \Gamma_{ij}(kp|(k-1)p)\}$
  $\lambda(k) = 0$
  $\tilde{\varphi}_{ij}(kp) = 2\arcsin(\tilde{d}_{ij}(kp)/2R)$ ▷ Sensor measurements
  $\Upsilon_{ij}(kp) := [\max\{\tilde{\varphi}_{ij}(kp) - \varphi_{\max}, 0\}, \min\{\tilde{\varphi}_{ij}(kp) + \varphi_{\max}, \varphi_v\}]$ ▷ Update
  for $l = 1{:}N^l$ **do**
    if $J_l(k|k-1) \cap \Gamma_{ij}(kp|(k-1)p)$ is a single interval **then**
      $\lambda(k) = \lambda(k) + 1$
    else if $J_l(k|k-1) \cap \Gamma_{ij}(kp|(k-1)p)$ is the union of two intervals **then**
      $\lambda(k) = \lambda(k) + 2$
    end if
  end for
  return $[\lambda(k), J_l(k|k-1) \cap \Gamma_{ij}(kp|(k-1)p)]$
end procedure

References

1. Ahmed, N., Cortes, J., Martinez, S.: Distributed control and estimation of robotic vehicle networks: overview of the special issue. IEEE Control Syst. Mag. **36**(2), 36–40 (2016)
2. Ariel, G., Ophir, Y., Levi, S., Ben-Jacob, E., Ayali, A.: Individual pause-and-go motion is instrumental to the formation and maintenance of swarms of marching locust nymphs. PLoS ONE **9**(7), e101636 (2014)
3. Bernard, M., Kondak, K., Maza, I., Ollero, A.: Autonomous transportation and deployment with aerial robots for search and rescue missions. J. Field Robot. **28**(6), 914–931 (2011)
4. Bopardikar, S.D., Englot, B., Speranzon, A.: Robust belief roadmap: planning under uncertain and intermittent sensing. In: 2014 IEEE International Conference on Robotics and Automation (ICRA), pp. 6122–6129. IEEE (2014)
5. Borenstein, J., Feng, L.: Measurement and correction of systematic odometry errors in mobile robots. IEEE Trans. Robot. Autom. **12**(6), 869–880 (1996)
6. Briñón-Arranz, L., Schenato, L., Seuret, A.: Distributed source seeking via a circular formation of agents under communication constraints. IEEE Trans. Control Netw. Syst. **3**(2), 104–115 (2015)
7. Chen, J., Sun, D.: Resource constrained multirobot task allocation based on leader-follower coalition methodology. Int. J. Robot. Res. **30**(12), 1423–1434 (2011)
8. Chen, Y.Q., Wang, Z.: Formation control: a review and a new consideration. In: 2005 IEEE/RSJ International Conference on Intelligent Robots and Systems, pp. 3181–3186. IEEE (2005)
9. Cho, B.S., Moon, W., Seo, W.J., Baek, K.R.: A dead reckoning localization system for mobile robots using inertial sensors and wheel revolution encoding. J. Mech. Sci. Technol. **25**(11), 2907–2917 (2011). https://doi.org/10.1007/s12206-011-0805-1
10. Couzin, I.D., Krause, J., Franks, N.R., Levin, S.A.: Effective leadership and decision-making in animal groups on the move. Nature **433**(7025), 513–516 (2005)
11. D'Amico, S., Montenbruck, O.: Differential GPS: an enabling technology for formation flying satellites. In: Sandau, R., Roeser, H.P., Valenzuela, A. (eds.) Small Satellite Missions for Earth Observation, pp. 457–465. Springer, Heidelberg (2010). https://doi.org/10.1007/978-3-642-03501-2_43
12. DeLellis, P., Garofalo, F., Iudice, F.L., Mancini, G.: Balancing cyclic pursuit using proximity sensors with limited range. IFAC Proc. Vol. **47**(3), 5784–5789 (2014)
13. DeLellis, P., Garofalo, F., Iudice, F.L., Mancini, G.: State estimation of heterogeneous oscillators by means of proximity measurements. Automatica **51**, 378–384 (2015)
14. DeLellis, P., Garofalo, F., Lo Iudice, F., Mancini, G.: Decentralised coordination of a multi-agent system based on intermittent data. Int. J. Control **88**(8), 1523–1532 (2015)
15. Dou, L., Song, C., Wang, X., Liu, L., Feng, G.: Coverage control for heterogeneous mobile sensor networks subject to measurement errors. IEEE Trans. Autom. Control **63**(10), 3479–3486 (2018)
16. Dudek, G., Jenkin, M.: Computational Principles of Mobile Robotics. Cambridge University Press, Cambridge (2010)
17. Elmaliach, Y., Agmon, N., Kaminka, G.A.: Multi-robot area patrol under frequency constraints. Ann. Math. Artif. Intell. **57**(3–4), 293–320 (2009). https://doi.org/10.1007/s10472-010-9193-y

18. Erdelj, M., Król, M., Natalizio, E.: Wireless sensor networks and multi-UAV systems for natural disaster management. Comput. Netw. **124**, 72–86 (2017)
19. Jetto, L., Longhi, S., Venturini, G.: Development and experimental validation of an adaptive extended Kalman filter for the localization of mobile robots. IEEE Trans. Robot. Autom. **15**(2), 219–229 (1999)
20. Le Bars, F., Sliwka, J., Jaulin, L., Reynet, O.: Set-membership state estimation with fleeting data. Automatica **48**(2), 381–387 (2012)
21. Lo Iudice, F., Acosta, J.A., Garofalo, F., DeLellis, P.: Estimation and control of oscillators through short-range noisy proximity measurements. Automatica **113**, 108752-1–108752-8 (2020)
22. Luo, R.C., Yih, C.C., Su, K.L.: Multisensor fusion and integration: approaches, applications, and future research directions. IEEE Sens. J. **2**(2), 107–119 (2002)
23. Mariottini, G.L., Morbidi, F., Prattichizzo, D., Pappas, G.J., Daniilidis, K.: Leader-follower formations: uncalibrated vision-based localization and control. In: Proceedings of the 2007 IEEE International Conference on Robotics and Automation, pp. 2403–2408. IEEE (2007)
24. Mwaffo, V., Curry, J.S., Iudice, F.L., De Lellis, P.: Pause-and-go self-balancing formation control of autonomous vehicles using vision and ultrasound sensors. IEEE Trans. Control Syst. Technol. **29**(6), 2299–2311 (2021)
25. Oh, K.K., Park, M.C., Ahn, H.S.: A survey of multi-agent formation control. Automatica **53**, 424–440 (2015)
26. Stroupe, A.W., Martin, M.C., Balch, T.: Distributed sensor fusion for object position estimation by multi-robot systems. In: Proceedings of the 2001 ICRA. IEEE International Conference on Robotics and Automation (Cat. No. 01CH37164), vol. 2, pp. 1092–1098. IEEE (2001)
27. Zabala, F., Polidoro, P., Robie, A., Branson, K., Perona, P., Dickinson, M.H.: A simple strategy for detecting moving objects during locomotion revealed by animal-robot interactions. Curr. Biol. **22**(14), 1344–1350 (2012)
28. Zhang, Q., Lapierre, L., Xiang, X.: Distributed control of coordinated path tracking for networked nonholonomic mobile vehicles. IEEE Trans. Ind. Inf. **9**(1), 472–484 (2012)